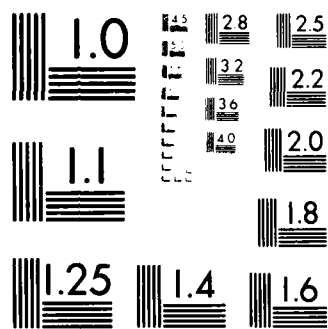


AD-A149 178

LOW CYCLE FATIGUE BEHAVIOR OF CONVENTIONALLY CAST MAR-M 1/1
200 AT 1000 C. (U) NATIONAL AERONAUTICS AND SPACE
ADMINISTRATION CLEVELAND OH LE. W W MILLIGAN ET AL.
SEP 84 NASA-E-2260 NASA-TM-83769 F/G 11/6 NL

UNCLASSIFIED





MICROCOPY RESOLUTION TEST CHART
NATIONAL BUREAU OF STANDARDS-1963-A

AD-A149 178

7

NASA
Technical Memorandum 83769

USAAVSCOM
Technical Report 84-C-16

Low Cycle Fatigue Behavior of Conventionally Cast MAR-M 200 at 1000° C

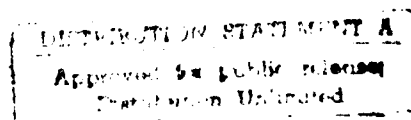
Walter W. Milligan
Georgia Institute of Technology
Atlanta, Georgia

and

Robert C. Bill
Propulsion Laboratory
AVSCOM Research and Technology Laboratories
Lewis Research Center
Cleveland, Ohio

September 1984

NASA



85 03 12 007

THE LOW CYCLE FATIGUE BEHAVIOR OF CONVENTIONALLY CAST MAR-M 200 AT 1000° C

Walter W. Milligan
Georgia Institute of Technology
Atlanta, Georgia 30332

and

Robert C. Bill
Propulsion Laboratory
AVSCOM Research and Technology Laboratories
Lewis Research Center
Cleveland, Ohio 44135

DTIC
ELECTE
JAN 14 1985
B

SUMMARY

The low cycle fatigue behavior of the nickel-based superalloy MAR-M 200 in conventionally cast form was studied at 1000° C. Continuous cycling tests without hold times, were conducted with inelastic strain ranges of from 0.04 to 0.33 percent. Tests were also conducted which included a hold time at peak strain in either tension or compression. For the conditions studied, it was determined that imposition of hold times did not significantly affect the fatigue life. Also, for continuous cycling tests, increasing or decreasing the cycle frequency did not affect life. Metallographic analysis revealed that the most significant damage mechanism involved environmentally assisted intergranular crack initiation and propagation, regardless of the cycle type. Changes in the γ' morphology (rafting and rod formation) were observed, but did not significantly affect the failure.

INTRODUCTION

High-temperature, low-cycle fatigue is a complex process that is studied from several different points of view. Many investigators are currently attempting to correlate actual physical damage mechanisms with observed quantitative fatigue behavior. An understanding of these physical mechanisms should be useful not only in life prediction, but also in alloy development and in materials applications situations. Gell and Leverant offer an excellent review of fatigue damage mechanisms in nickel-based superalloys (ref. 1).

A recently developed life prediction technique that is useful in gaining an understanding of physical mechanisms is the Strainrange Partitioning (SRP) approach (ref. 2). In this approach the effects of creep and plasticity, and their interactions with each other can be documented. The SRP approach has gained fairly wide acceptance as a framework for low cycle fatigue testing. One possible drawback to SRP, however, is that environmental degradation can sometimes be mistaken for creep damage.

In this study, a turbine blade alloy, MAR-M 200, was investigated (primarily at 1000° C) to try to identify relevant physical damage mechanisms. The objective was to relate observed microstructural changes to the process of crack initiation and fatigue life, and to provide an experimental and mechanistic basis against which results obtained from more complex nonisothermal cycling experiments might be compared.

DISTRIBUTION STATEMENT A

Approved for public release
Distribution Unlimited

MATERIAL

MAR-M 200 is a cast nickel-based superalloy originally developed for turbine blade application. The composition is outlined in table I. The microstructure consists of approximately 60 vol% primary γ' in a γ matrix, with both $M_{23}C_6$ and MC type carbides. The alloy was conventionally cast into solid "hourglass" specimens as illustrated in figure 1, which resulted in a radial grain structure with grain sizes of approximately 1 mm by 2 to 3 mm. The specimens were tested in the as cast and machined condition.

APPARATUS AND PROCEDURE

Testing was conducted on a closed-loop, servohydraulic test system, in the diametral strain-controlled mode (ref. 3). Specimens were heated using a direct resistance unit. The "hourglass" specimen design is shown in figure 1.

First, to establish the conventional Coffin-Manson relationship, isothermal, continuous cycling (PP type) tests were conducted at 1000° C in the fully reversed, strain controlled mode. The tests were conducted at a frequency of 0.5 Hz, with plastic strain ranges from 0.04 to 0.33 percent. Next, a series of tests was conducted at a constant inelastic strain range of 0.2 percent with varying cycle parameters: continuous cycling tests were conducted at frequencies of 0.033 and 1.00 Hz; CP tests, which included a 2.5 min hold time at the maximum tensile strain, and a PC test, which included a 2.5 min hold time at the maximum compressive strain, were also conducted. Finally, several PP type tests were conducted at lower temperatures (870° and 760° C). A metallographic and fractographic study was undertaken to identify damage mechanisms. Also, a study of oxidation and diffusion was conducted to help clarify the role of the environment. This consisted of exposing samples under no load in air at 1000° C for periods ranging from 15 min to 96 hr. The samples were sectioned, mounted in mineral filled epoxy (for good edge retention), polished, and documented metallographically.

RESULTS

Life Relationships

As seen from figure 2, the strain-controlled fatigue data are fairly consistent, and the alloy follows the Coffin-Manson Law in the range of inelastic strainrange ($\Delta\epsilon_{in}$) studied. Also, for the conditions studied ($\Delta\epsilon_p = 0.2$ percent, $T = 1000^\circ\text{C}$), the fatigue life is not affected by changing the frequency or imposing a hold time. Results from SRP tests of hollow tubular MAR-M-200 specimens reported by Manson, Halford and Oldrieve (ref. 4) at 927° C are also shown for comparison. An approximately fourfold increase in life is seen for the 1000° C data compared to the 927° C results from reference 4. This is believed to be due to two effects. First, consider the mechanical properties. For a given inelastic strain range, peak stresses at 1000° C are about 25 percent lower than those at 927° C, thereby reducing the dynamic crack growth driving force. Also, ductility of MAR-M 200 at 1000° C is 10 to 20 percent higher than at 927° C, thereby increasing the low cycle fatigue life one would predict on the basis of cyclic inelastic strain. Second, all other

things being equal, the lives of hollow tube specimens are observed to be somewhat lower than those of solid specimens (as used in the present investigation), consistent with the general observation of crack initiation on the inner surface of the hollow tube specimens.

Crack Initiation and Propagation

At 1000° C, crack initiation always occurred in grain boundaries on the specimen surface, as shown in figures 3 to 6. It was also observed that crack initiation was always accompanied by preferential oxidation and alloy depletion at the grain boundary.

In all tests that included a hold time, crack propagation at 1000° C was 100 percent intergranular. In continuous cycling (PP type) tests, crack propagation at 1000° C was observed to be mixed intergranular and transgranular with the intergranular mode being the most dominant as illustrated in figures 4 and 5. The highest degree of transgranular cracking was observed in Specimen G2, a PP type test (Frequency = 1 Hz), in which about 25 percent of the the cracking present was transgranular. At 870° C and 760° C, however, transgranular propagation became much more dominant.

Oxidation Behavior

The samples that were oxidized under no load were compared to the fatigued specimens metallographically. The degree of oxidation and depletion was inhomogeneous, due possibly to differences in the adherence of the oxide scale in grains of different orientation, or to dendritic segregation. It was determined, however, that the rates of oxidation, alloy depletion, and intergranular attack are essentially a function of time only, and not of the loading history. There was one notable exception, as illustrated in figure 6. Although the degree of diffusion and oxidation was about the same for the fatigued sample and the unstressed sample, the oxide scale tended to "grow" into the base metal grain boundary during fatigue. In the unstressed samples, oxide "spikes" were nucleated in the alloy depletion zones, but the scale itself did not appear to be continuous. (The "spikes" were also nucleated in the depleted zones of the fatigued samples.)

Microstructural Instabilities

In addition to surface reactions (oxidation and alloy depletion), the bulk microstructure of the alloy changed during the fatigue process at 1000° C. As shown in figure 7, a tensile strain hold time (CP type test) induced "rafting," which is an elongating and coalescing of the γ' particles in the $\langle 100 \rangle$ crystallographic direction most nearly perpendicular to the tensile axis. A compressive strain hold time (PC type test) induced directional coarsening in the $\langle 100 \rangle$ crystallographic direction most nearly parallel to the tensile axis. These phenomena are very inhomogeneous, depending strongly on grain orientation relative to the tensile axis. The γ' morphology of many grains changed very little, even during the longest CP type test.

In the continuous cycling (PP type) tests, and in the unstressed samples, very slight γ' coarsening in random $\langle 100 \rangle$ directions was observed.

DISCUSSION

The SRP behavior of polycrystalline MAR-M 200 at 1000° C is typical of high γ' Nickel-based superalloys used in turbine airfoil applications. These materials were designed for creep resistance, and by additions of boron, zirconium, carbon, and carbide formers, grain boundary sliding has been virtually eliminated. For this reason, the moderate to high inelastic strain ranges imposed resulted in CP and PC lives that were about the same as the PP lives. This type of behavior has been documented for MAR-M 200 at 927° C, (ref. 4) for Rene' 80 (which is microstructurally and chemically very similar to MAR-M 200) at 1000° C, (ref. 5) and for other similar alloys.

Although grain boundary sliding has been eliminated, other creep processes have not been. In the CP and PC type tests, the partitioned (ref. 2) inelastic strain ranges consist of 40 to 50 percent CP or PC type inelastic strain. Also, the constant inelastic strain range continuous cycle tests (PP type) illustrate that creep can occur even during this type of cycle. As the continuous cycle frequency was increased from 0.033 to 1.00 Hz, the stress range (for the same inelastic strain range) increased from 550 to 680 MPa. This indicates that a dynamic stress relaxation creep mechanism is active. The probable creep mechanisms involved are dislocation climb and bulk diffusion.

Although creep is taking place, it does not significantly affect the fatigue life under the conditions studied. The reason for this is that the cracking occurs in the grain boundaries, while the creep deformation processes appear to be occurring within the grains.

One side effect of the creep-fatigue deformation process is the directional coarsening or rafting, of the γ' particles. This behavior has been reported for single crystal superalloys, (ref. 6) and recent investigations have suggested that "rafting" may be beneficial for creep resistance. In the conventionally cast form, however, the creep-fatigue lives appear to be independent of this behavior. Once again, the intergranular nature of the cracking seems to be the reason.

The primary damage mechanism for this material at 1000° C consists of environmentally assisted intergranular crack initiation and propagation, as illustrated in figures 5 and 6. Gell and Leverant (ref. 1), McMahon and Coffin (ref. 7), Coffin (ref. 8), and Antolovich, Liu and Baur (ref. 9) have documented this type of behavior for similar alloys at high temperature. Several specific mechanisms have been proposed. Gell and Leverant describe an oxidation affected zone ahead of the intergranular crack. The oxidation affected zone is structurally and chemically changed, specifically undergoing depletion of oxide forming elements. Under some circumstances intergranular crack growth may be accelerated by the formation of this oxidation affected zone ahead of the crack. An intergranular crack initiation mechanism was observed by McMahon and Coffin in cast Udimet 500 wherein surface oxide ridges that formed at highly stressed grain boundary sites led to crack initiation. McMahon and Coffin also observed extensive oxide penetration, independent of cracking, along surface connected grain boundaries as well as alloy depletion adjacent to

the grain boundaries. In studies performed on Rene' 80, Coffin again observed crack initiation at surface grain boundary sites where oxide ridging occurred. However, crack propagation in Rene' 80 was primarily transgranular, independent of cyclic loading frequency. Antolovich et. al. reported crack initiation in Rene' 80 at deeply penetrating oxide spikes that formed in surface connected grain boundaries. An oxidation controlled crack initiation life prediction method was proposed to account for these observations.

In addition to the mechanistic observations cited above, phenomenological support for the effect of the environment has been found in the literature. Halford and Nachtigall (ref. 5) investigated the low cycle fatigue behavior of Rene' 80 at 1000° C in air, and found essentially the same behavior as documented here for MAR-M 200. The four SRP lifelines coincided. Kortovich and Sheinker (ref. 10) studied Rene' 80 from the same heat at 1000° C in a high vacuum. Fatigue lives were improved drastically (approximately doubled) for the PP type cycle in vacuum compared to air, resulting in a separation of the SRP lifelines. They reported that crack propagation at 1000° C in vacuum for the PP cycle was essentially transgranular, while CP and PC type cycles still resulted in intergranular cracking. The major effect of the environment seems to be a promotion of intergranular fracture, even in PP type tests, resulting in lower fatigue lives.

Thus, the results obtained here for polycrystalline MAR-M 200 are generally consistent with those for other conventionally cast nickel based superalloys. An interesting observation pertaining to MAR-M 200 however, is the insensitivity of cyclic crack growth rate to the mode of crack propagation (intergranular or mixed transgranular/intergranular), resulting in cyclic lives that were independent of the cycle type. The key role played by oxidation in the crack initiation and early propagation process provides a basis for better understanding the strong sensitivity of cyclic life to the phase relationship between the thermal cycle and the mechanical cycle seen in the thermomechanical fatigue experiments reported in reference 11. Because of crack opening under tensile loading at high temperatures, there was much more opportunity for oxidation mechanisms to promote crack growth under in-phase cycling (tensile load at maximum temperature) than under out-of-phase cycling (compressive load at maximum temperature).

CONCLUSIONS

1. For the conditions investigated ($T = 1000^{\circ} \text{C}$, inelastic strain range < 0.05 percent $\nu < 1 \text{ Hz}$), the fatigue life (N_f) of conventionally cast MAR-M 200 is not significantly affected by frequency or hold times.
2. The most significant damage mechanism in this region, regardless of cycle type, consists of oxidation accelerated intergranular crack initiation and propagation.
3. Damaging microstructural changes observed included preferential oxidation and alloy depletion immediately adjacent to the grain boundaries. Changes in the bulk microstructure observed included rafting, rod formation, and γ' coarsening, none of which seemed to have a significant effect on the fatigue life (N_f).

REFERENCES

1. Gell, M.; and Leverant, G. R.: Mechanisms of High Temperature Fatigue. Fatigue at Elevated Temperature. ASTM STP 520, 1972, pp 37-67.
2. Hirschberg, Marvin H.; and Halford, Gary R.: Use of Strainrange Partitioning to Predict High-Temperature Low-Cycle Fatigue Life. NASA TN D-8072, 1976.
3. Hirschberg, M. H.: A Low Cycle Fatigue Testing Facility. Manual on Low Cycle Fatigue Testing. ASTM STP 465, 1969, pp 67-86.
4. Manson, S. S.; Halford, G. R.; and Oldrieve, R. E.: Relation of Cyclic Loading Pattern to Microstructural Fracture in Creep Fatigue. NASA TM-83473, 1983.
5. Halford, G. R.; and Nachtigall, A. J.: Strainrange Partitioning Behavior of the Nickel-Base Superalloys, Rene' 80 and In 100. Characterization of Low Cycle High Temperature Fatigue by the Strainrange Partitioning Method. AGARD-CP 243, 1978, pp. 2-1 - 2-14.
6. Lien, J. K.; and Copley, S. M.: The Effect of Uniaxial Stress on the Periodic Morphology of Coherent Gamma Prime Precipitates in Nickel-Base Superalloy Crystals. Metall. Trans., vol. 2, no. 1, Jan. 1971, pp 215-219.
7. McMahon, C. J.; and Coffin, L. F.: Mechanisms of Damage and Fracture in High-Temperature, Low-Cycle Fatigue of a Cast Nickel-Based Superalloy. Metall. Trans., vol. 1, no. 12, Dec. 1970, pp 3443-3450.
8. Coffin, L. F. Jr.: The Effect of Frequency on the Cyclic Strain and Fatigue Behavior of Cast Rene' at 1600° F. Metall. Trans., vol. 5, 1974, no. 5, May pp 1053-1060.
9. Antolovich, Stephen D.; Liu, S.; and Baur, R.: Low Cycle Fatigue Behavior of Rene' 80 at Elevated Temperature. Metall. Trans. A, vol. 12, no. 3, Mar. 1981, pp 473-481.
10. Kortovich, C. S.; and Sheinker, A. A.: A Strainrange Partitioning Analysis of Low Cycle Fatigue of Coated and Uncoated Rene' 80. Characterization of Low Cycle High Temperature Fatigue by the Strainrange Partitioning Method. AGARD-CP-243, 1978, pp. 1-1 - 1-23.
11. Bill, Robert C., et al.: Preliminary Study of Thermomechanical Fatigue of Polycrystalline MAR-M 200. NASA TP-2280, 1984.

TABLE I. - MAR-M 200 ALLOY COMPOSITION (wt %)

NI	Al	Ti	Co	W	Cr	Cb	C	Fe	Zr	B	S	Si	Cu	Mn
Bal.	5.2	2.1	10.3	12.6	9.2	1.0	0.12	0.6	0.043	0.015	0.003	0.073	<0.1	<0.02

TABLE II. - FATIGUE TEST DATA FOR POLYCRYSTALLINE MAR-M 200 AT 1000° C

Specimen	Cycle type ^a	Frequency, Hz	Total stress range, MPa	Total strain range, x10 ² cm/cm	Inelastic strain range, x10 ² cm/cm	Number of cycles to failure, N _f
HH33	PP	0.50	370	0.27	0.04	11 800
HH54	PP	.50	425	.30	.07	4 060
HH69	PP	.50	385	.28	.07	15 400
HH49	PP	.50	500	.38	.09	1 960
G25	PP	.50	625	.48	.15	950
G24	PP	.033	550	.44	.20	320
G30	PP	.50	660	.50	.20	520
HH41	PP	.50	600	.43	.20	760
HH44	PP	.50	630	.46	.21	335
G2	PP	1.00	680	.57	.20	630
HH48	PP	.50	625	.46	.28	340
HH18	PP	.50	730	.53	.33	195
G14	CP	^b .50	690	.47	.22	450
G8	CP	^b .50	630	.43	.20	760
G27	PC	^b .50	610	.46	.20	380

^aPP denotes a continuous test with no hold time. CP denotes a test that includes a hold time at the maximum tensile strain. PC denotes a test that contains a hold time at the maximum compressive strain.

^bThese tests included a 2.5 min hold time, with a 2 sec (0.5 Hz) reversal.

Accession For	
NTIS GRA&I	<input checked="" type="checkbox"/>
DTIC TAB	<input type="checkbox"/>
Unannounced	<input type="checkbox"/>
Justification	
By	
Distribution /	
Availability Codes	
Dist	
A-1	



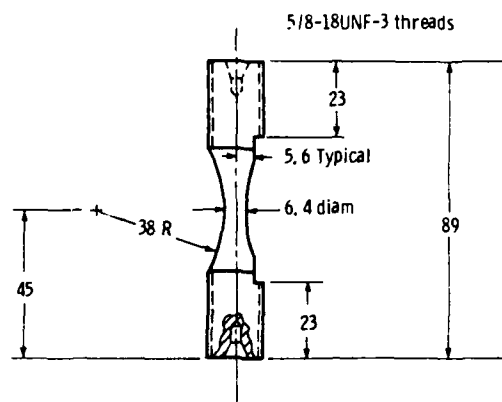


Figure 1. - Specimen geometry. (Note: all dimensions are in millimeters (except threads).)

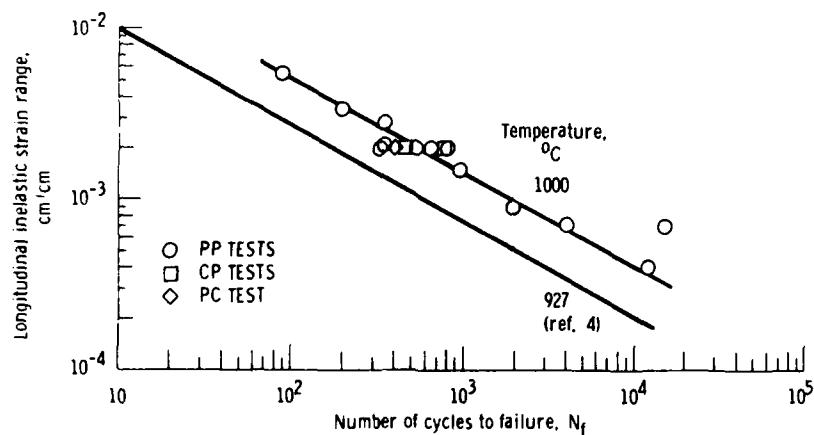
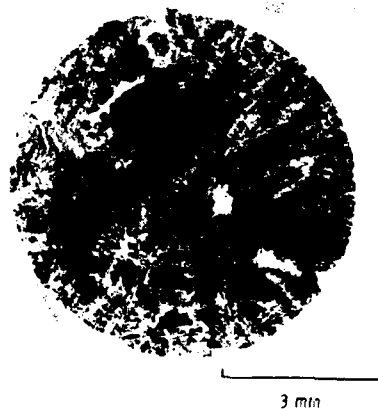
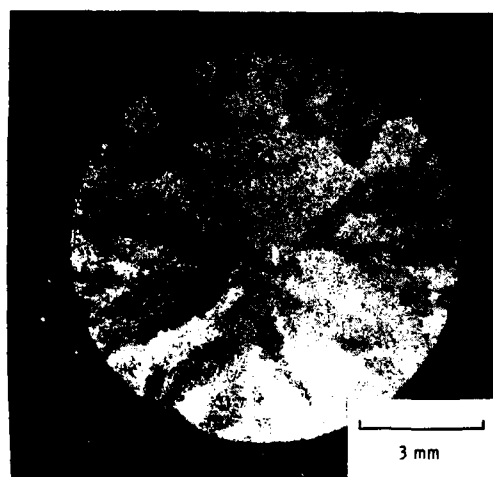


Figure 2. - Inelastic strain range versus N_f for polycrystalline MAR-M 200 at 1000°C.



(a) Fracture surface of specimen G30 (no hold time).



(b) Polished and etched section of specimen G30.

Figure 3. - Photographs illustrating the intergranular nature of cracking.

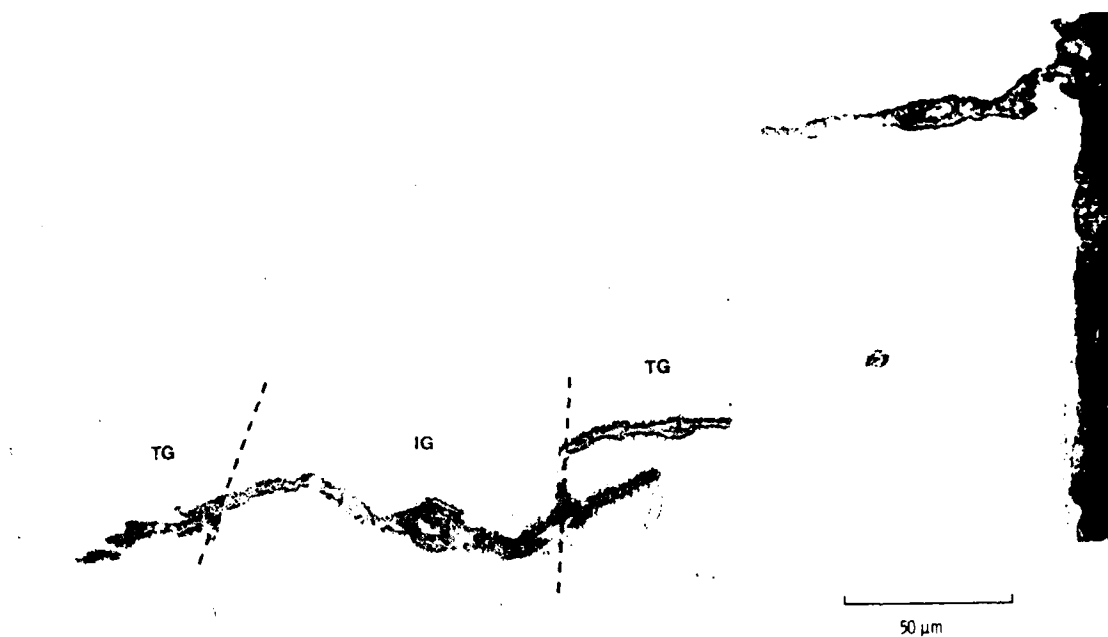
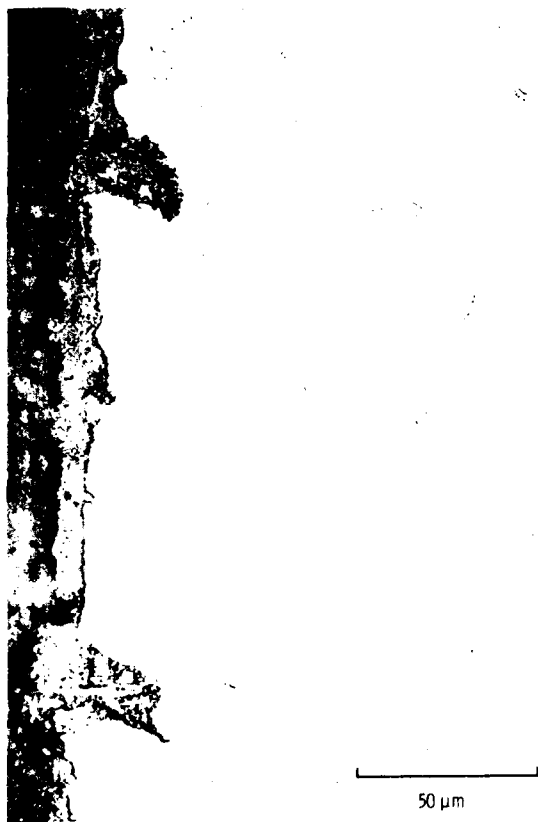


Figure 4. - Photomicrograph showing mixed-mode crack propagation, specimen G30. The upper crack initiated in the grain boundary and propagated transgranularly. The lower crack is surface-connected, below the plane of view.



Figure 5. - Photomicrograph showing the crack front propagating through a grain boundary. Specimen G14 (tensile strain holds).

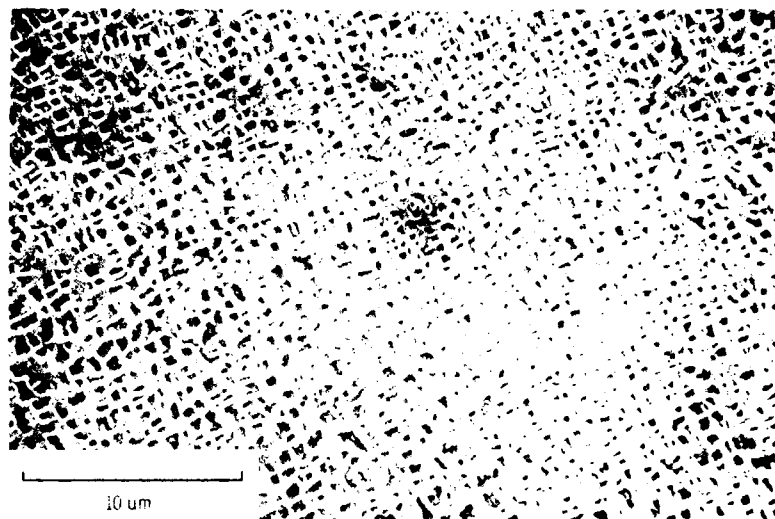


(a) Specimen 627 (compressive strain hold, $t_f = 17$ hr). Note the crack initiated at the lower grain boundary.

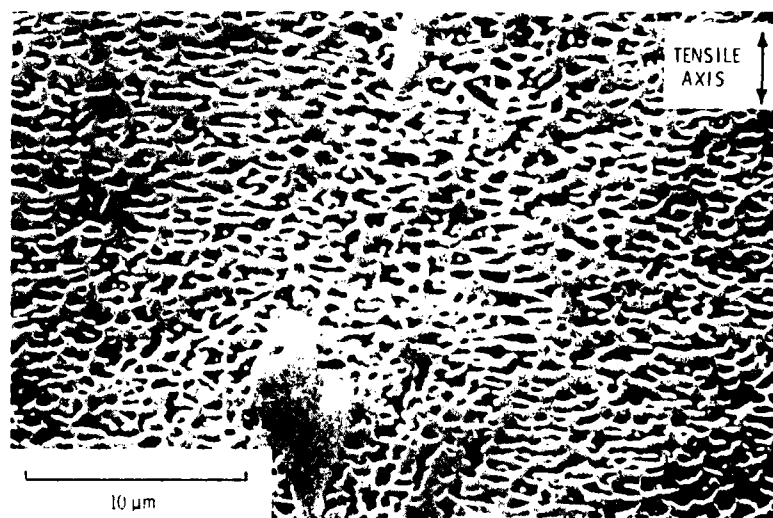


(b) Sample oxidized under no load for 16 hours.

Figure 6. - Preferential oxidation and diffusion at grain boundaries.

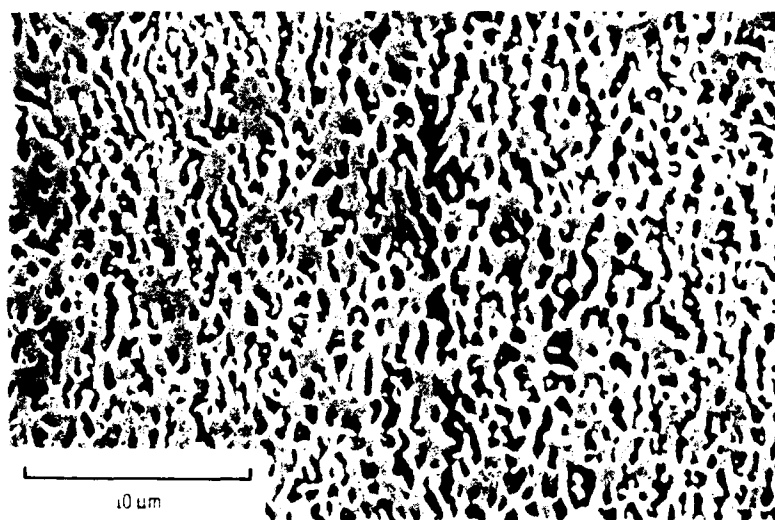


(a) Untested (starting) microstructure.



(b) Specimen G14 (tensile strain hold).

Figure 7. Scanning electron micrographs illustrating the changes in γ' morphology due to creep fatigue.



(c) Specimen G27 (compressive strain hold).

Figure 7. - Concluded.

1. Report No NASA TM-83769 USAAVSCOM-TR-84-C-16		2. Government Accession No. <i>AD A149128</i>		3. Recipient's Catalog No.	
4. Title and Subtitle Low Cycle Fatigue Behavior of Conventionally Cast MAR-M 200 at 1000° C				5. Report Date September 1984	
				6. Performing Organization Code 505-33-22	
7. Author(s) Walter W. Milligan and Robert C. Bill				8. Performing Organization Report No. E-2260	
				10. Work Unit No.	
9. Performing Organization Name and Address NASA Lewis Research Center and Propulsion Laboratory U.S. Army Research and Technology Laboratories (AVSCOM) Cleveland, Ohio 44135				11. Contract or Grant No.	
				13. Type of Report and Period Covered Technical Memorandum	
12. Sponsoring Agency Name and Address National Aeronautics and Space Administration Washington, D.C. 20546 and U.S. Army Aviation Systems Command, St. Louis, Mo. 63120				14. Sponsoring Agency Code	
15. Supplementary Notes Walter W. Milligan, Georgia Institute of Technology, Atlanta, Georgia 30332; Robert C. Bill, Propulsion Laboratory, AVSCOM Research and Technology Laboratories, Lewis Research Center, Cleveland, Ohio 44135.					
16. Abstract The low cycle fatigue behavior of the nickel-based superalloy MAR-M 200 in conventionally cast form was studied at 1000° C. Continuous cycling tests, without hold times, were conducted with inelastic strain ranges of from 0.04 to 0.33 percent. Tests were also conducted which included a hold time at peak strain in either tension or compression. For the conditions studied, it was determined that imposition of hold times did not significantly affect the fatigue life. Also, for continuous cycling tests, increasing or decreasing the cycle frequency did not affect life. Metallographic analysis revealed that the most significant damage mechanism involved environmentally assisted intergranular crack initiation and propagation, regardless of the cycle type. Changes in the γ' morphology (rafting and rod formation) were observed, but did not significantly affect the failure.					
17. Key Words (Suggested by Author(s)) Fatigue High temperature Oxidation Superalloy				18. Distribution Statement Unclassified - unlimited STAR Category 26	
19. Security Classif (of this report) Unclassified		20. Security Classif (of this page) Unclassified		21. No. of pages	
				22. Price*	

END

FILMED

2-85

DTIC